



Efficient Spectral Method for Stable Stratified Power-Law Fluid Flows with Dispersion Over Convectively Heated Truncated Cone in a Non-Darcy Porous Medium

Ch. RamReddy¹ · Abhinava Srivastav¹

Accepted: 7 May 2021 / Published online: 16 May 2021

© The Author(s), under exclusive licence to Springer Nature India Private Limited 2021

Abstract

This problem deals with the power-law fluid flow with thermally stable stratification in a non-Darcy porous medium over a convectively heated truncated cone and this work is very useful in actual and applied circumstances due to presence of non-linear Boussinesq approximation. The combined thermal diffusivity is taken as the addition of molecular diffusivity and diffusivity related to mechanical dispersion. Local non-similarity technique and spectral local linearization method are applied to solve the governing equations. A convergence test for this scheme is performed and validation of methodology is given by comparing the results in special cases with already established results. It is noted that the proposed combined scheme is an efficient algorithm with faster convergence and it acts as an alternative tool for regular numerical techniques to solve non-linear boundary value problems that occur frequently in industrial and engineering applications. The major conclusion of this study is that the magnitude of skin friction coefficient and Nusselt number are very much influenced with the presence and absence of Biot number, thermal stratification and thermal dispersion for the power-law fluids and strongly depend on the non-linear density temperature parameter.

Keywords Non-similarity solutions · Spectral local linearization method · Stratified power-law fluid · Non-Darcy porous medium · Convectively heated truncated cone

Introduction

A medium (or material) which contains voids is termed as porous medium and its skeletal portion is usually called the frame or matrix. In general, a fluid (liquid or gas) is typically filled in these pores and any porous medium is normally distinguished by porosity described in terms of ratio of void space volume over total volume (between 0 and 1). Examples of porous media are very wide, ranging from natural substances (e.g., soil, rocks and biological tissues) to artificial substances (e.g., cements, ceramics) and different properties of these materials are only rationalized by treating them as porous media. Porous medium concept is used

✉ Ch. RamReddy
chittetiram@gmail.com

¹ Department of Mathematics, National Institute of Technology, Warangal Pin Code-506004, T.S., India

in different areas of engineering and applied science, for example, petroleum, construction or material science, filtration, geo-mechanics, soil mechanics, acoustics, etc. Flow of fluids (Newtonian or non-Newtonian) through porous matrix exerts a huge amount of interest among researchers and has emerged as a separate area of research. For example, it can be helpful in controlling environment pollution by finding moisture and temperature distribution in agricultural lands. Liu *et al.* [1] provided the finite element approach and its theoretical predictions for non-linear boundary value problem which is utilized to formulate the non-Fickian flow of fluid in porous media. Therefore, development and analysis of various fluid models are given to study the flow properties in non-Darcy porous media in different books (Ref. [2–4]).

The viscosity in two type of power-law fluids, shear thinning (pseudoplastic) and shear thickening (dilatant), decreases and increases with stress respectively. Due to wide application of power-law fluids in modern science and technology, Shenoy [5] and Cheng [6] studied influences of important parameters for applicable geometries. Mandal *et al.* [7] provided a numerical solution for the fluid models of pulsatile blood flow between an irregular stenosed arterial segment which is very useful in the areas related to medical science and research. The role of local production of thermal energy through viscous stress mechanism of power-law fluid flow due to buoyancy forces is studied by Khidir *et al.* [8]. Kairi [9] has shown that the increment in the radius of slender paraboloid in a porous medium reduces the Nusselt number for all shear thickening and thinning fluids.

Due to significance of the thermal stratification and its involvement in the major applications as heat exchangers used in domestic hot water tank, the study of thermal stratification in different porous media concepts has gained notable importance in modern times. The experimental and analytical results related to thermal stratification in lakes are given by Dake and Harleman [10]. From Knudsen and Furbo [11], one can get ideas about the use of heat exchangers in the storage tank and solar collector. In view of these applications, Narayana *et al.* [12] and Cheng [13] conducted independent studies on the free convective flow over vertical flat plate and vertical wavy surface, respectively, with dilatant and pseudoplastic fluids and concluded that the total Nusselt number value for wavy surface is more in comparison to the smooth surface. On the other hand, thermal dispersion effect plays a vital role due to inertial effect existence in a non-Darcy porous medium. In non-uniform geometries, particularly in the packed beds, flow of fluid through curvy paths led to the thermal dispersion at the pore level of the involved porous media. Several researchers, to point out few, Cheng [14] and Plumb [15], analysed different fluid flows and heat transfer with thermal dispersion. Hong *et al.* [16] treated $\frac{\chi du_{\infty}}{\alpha} = \chi Pe_{\chi}$ as Ds and then explained the flow analysis theoretically. By adopting the similar representations, Kairi and Murthy [17] conducted the study of free convective flows of dilatant or pseudoplastic fluids with thermal stratification and dispersion. Numerical study for the same fluid flow but without prescribing the temperature and concentration on the vertical surface, is presented by Srinivasacharya *et al.* [18] and concluded that the obtained similarity solutions are valid only for small values of X - location (i.e. $0 < X < 1$). Later, Vasu *et al.* [19] performed an entropy generation analysis for stratified flow along vertical surface (for elaborative discussions, see the citations therein).

In recent times, various real life flow applications are dealt in emerging scientific and technological areas and the nature of these flows are very complex, consequently the study related to heat transfer mechanism is also very tough. So convective boundary conditions are very important for this kind of flows, usually occurring in nuclear reactors, solar collectors etc. The similarity solutions of free convective power-law fluid flow past a convectively heated vertical surface are obtained by Ece and Buyuk [20]. Yao *et al.* [21] discussed the

convective transport along shrinking and/or stretching wall problem. Many thermal systems operated at very high temperatures suffer the loss of its linear nature of density-temperature relation given by $\rho - \rho_\infty + \rho_\infty \beta_0 (T - T_\infty) = 0$ (For more details, one can refer Pop and Ingham [3]). This gives the idea of non-linear Boussinesq approximation or non-linear convection where it has $\rho - \rho_\infty + \rho_\infty \beta_0 (T - T_\infty) \left[1 + \frac{\beta_1 (T - T_\infty)}{\beta_0} \right] = 0$ (Refer Partha [22] and its citations). A strong influence of this non-linearity is noticed on different fluid flow problems. The impact of dispersion on the non-linear convective flow of incompressible shear thickening and thinning fluids is investigated by RamReddy *et al.* [23] and it is concluded that the velocity and local Nusselt number are increased when the increment takes place in D_s parameter. But a detailed idea regarding the rates of flow as well as heat transfer of these dilatant and pseudoplastic fluids is yet to emerge.

Many engineering and industrial problems e.g., processing of melted plastics at a large level, edible items or slurries and polymers etc., require free convective power-law fluid flow from truncated cones subjected to the convective boundary condition in porous media. But from available literature, it is observed that this model is not studied so far although results of these kind of studies can serve as a useful productive tool to solve important engineering and industrial problems. There are some works available in the literature, namely, Na and Chiou [24], Gorla *et al.* [25], Cheng [26,27] but these papers are only related to power-law fluid flow over truncated cone maintained at uniform wall temperature and/or subject to uniform heat flux conditions. This motivates us to analyze the above-said fluid flow problem in detail as it helps us to study various effects like: (i) ratio of internal thermal resistance of truncated cone surface to the thermal resistance of boundary layer in terms of Biot number, and (ii) effectiveness of non-uniform pore level velocity over temperature field within the specific porous medium in terms of thermal dispersion parameter. So, in this article, the natural convective flow over truncated cone in a power-law fluid saturated non-Darcy porous medium is mathematically modelled and then the associated governing equations are solved using non-similarity technique and spectral local linearization method. Later, the results are graphically analyzed in detail along with their proper physical significance and real life applications as seen in the cooling of magmatic intrusion or radioactive sub-surface storage location which involve convective transport theory.

Mathematical Formulation and Analysis

Figure 1 displays a mathematical configuration to study the natural convective flows related to thermally stratified dilatant and pseudoplastic fluids along a convectively heated truncated cone. The non-Darcian type of porous medium is taken in this analysis. The coordinate axes x and y are in the parallel and perpendicular directions to the truncated cone and x_0 is the distance between its leading edge and origin O . Here, $\bar{x} = x - x_0$ is considered as modified streamwise coordinate, T_f is the fluid temperature and $T_\infty(\bar{x}) = T_{\infty,0} + A^* \bar{x}$ is the temperature of the linearly stratified ambient medium which generates a stable thermal stratification. The stratification intensity is controlled by a parameter A^* . This steady, two dimensional and laminar fluid flow is in thermodynamic equilibrium with porous medium. Also, to neglect boundary effect and apply the Forchheimer flow model, permeability of the medium is taken less with moderate flow intensity. In addition, there is notable significance of large changes in the temperatures of ambient medium and surface of the truncated cone.

It is also presumed that the thickness of momentum and thermal boundary layer is very less compared to the local radius of truncated cone. The approximation $r = x \sin A$ [See

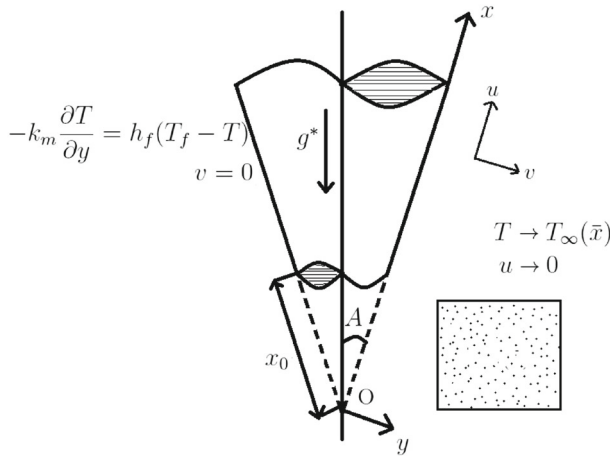


Fig. 1 Geometry used in the problem

Singh *et al.* [28] shows the relation between truncated cone radius and local radius at a point situated in the boundary layer which implies $x_0 < x < \infty$ as the region in which governing equations and boundary conditions are valid. Hence, these assumptions are practical and more relevant.

So, the governing equations along with boundary conditions associated with this fluid flow model can be written as

$$\frac{\partial(ru)}{\partial x} + \frac{\partial(rv)}{\partial y} = 0 \tag{1}$$

$$\frac{\partial u^n}{\partial y} + \frac{bK^*}{v} \frac{\partial u^2}{\partial y} = \frac{K^* g^*}{v} \left\{ [\beta_0 + 2\beta_1(T - T_\infty(\bar{x}))] \frac{\partial T}{\partial y} \right\} \cos A \tag{2}$$

$$u \frac{\partial T}{\partial x} + v \frac{\partial T}{\partial y} = \frac{\partial}{\partial y} \left(\alpha_* \frac{\partial T}{\partial y} \right) \tag{3}$$

$$\begin{aligned} v = 0, \quad -k_m \frac{\partial T}{\partial y} &= h_f(T_f - T), \quad \text{at } y = 0 \\ u \rightarrow 0, \quad T &\rightarrow T_\infty(\bar{x}) \quad \text{as } y \rightarrow \infty \end{aligned} \tag{4}$$

where g^* is the acceleration due to gravity, h_f is the convective heat transfer coefficient, k_m is the thermal conductivity, v is the kinematic viscosity, A is the inclination of angle, T is the temperature, b is the empirical constant and (u, v) are the Darcian velocities. A quantity α_* is obtained by taking the sum of $\alpha_d = \chi ud$ (thermal diffusivity) and α (molecular diffusivity) as per Plumb [15], where χ is the mechanical dispersion coefficient and d is the pore diameter. Next, β_0 and β_1 are the 1st and 2nd order thermal expansion coefficients respectively. When $n = 1$ (the power-law index), the fluid becomes Newtonian and for $n > 1$ and $n < 1$, the fluid is dilatant and pseudoplastic respectively. K^* denotes the modified permeability of the porous medium which is a function of n (See [29] and [30] for more details).

The stream function ψ is introduced in such a way that it satisfies the equation of continuity (1) i.e., $u = \frac{1}{r} \frac{\partial \psi}{\partial y}$, $v = -\frac{1}{r} \frac{\partial \psi}{\partial x}$. The non-dimensional relations utilized to get the non-dimensional form of Eqs.(2)-(4) are

$$\xi = \frac{\bar{x}}{x_0}, \quad \eta = \frac{y}{\bar{x}} Ra^{\frac{1}{2}}, \quad f(\xi, \eta) = \frac{Ra^{-\frac{1}{2}}}{\alpha r} \psi(\xi, \eta), \quad \theta(\xi, \eta) = \frac{T(\xi, \eta) - T_{\infty}(x - x_0)}{(T_f - T_{\infty,0})} \tag{5}$$

where $Ra = \frac{\bar{x}}{\alpha} \left(\frac{\rho \beta_0 g^* K^* \cos A (T_f - T_{\infty,0})}{\mu} \right)^{\frac{1}{n}}$ is the local modified Darcy-Rayleigh number.

Using these transformations (5) in the Eqs. (1) to (3), the non-dimensional form of the above equations become

$$\left[n (f')^{n-1} + 2 Gr^* f' \right] f'' = (2\alpha_1 \theta + 1) \theta' \tag{6}$$

$$\theta'' + (f' \theta'' + f'' \theta') Ds + \left(\frac{\xi}{\xi + 1} + 0.5 \right) f \theta' - S_T \xi f' = \xi f' \frac{\partial \theta}{\partial \xi} - \xi \frac{\partial f}{\partial \xi} \theta' \tag{7}$$

The boundary conditions (4) in their transformed forms can be written as

$$\begin{aligned} 2 \xi (\xi + 1) \left(\frac{\partial f}{\partial \xi} \right)_{\eta=0} + (3 \xi + 1) f(\xi, 0) &= 0, \\ \theta'(\xi, 0) - Bi \xi^{\frac{1}{2}} [\theta(\xi, 0) - 1 + S_T \xi] &= 0, \\ f'(\xi, \eta) \rightarrow 0, \quad \theta(\xi, \eta) \rightarrow 0 \quad \text{as } \eta \rightarrow \infty. \end{aligned} \tag{8}$$

Here prime indicates the differentiation in respect of η and $Gr^* = \frac{b K^*}{\nu} \left(\frac{\alpha Ra}{\bar{x}} \right)^{2-n}$, $\alpha_1 = \frac{\beta_1}{\beta_0} (T_f - T_{\infty,0})$, $Ds = \frac{\chi d Ra}{\bar{x}}$, $S_T = \frac{A^* x_0}{(T_f - T_{\infty,0})}$, $Bi = \frac{h_f \sqrt{\bar{x}_0}}{k_m} \left(\frac{\bar{x}}{Ra} \right)^{\frac{1}{2}}$ represent the modified Grashof number, non-linear density-temperature parameter, thermal dispersion parameter, thermal stratification parameter and Biot number respectively. When $\xi \rightarrow 0$ (i.e., $x \rightarrow x_0$), this problem is converted to flow problem past a vertical plate. Similarly, when $x_0 = 0$, ξ becomes very large which is utilized to obtain the same problem with full cone as a geometry.

Non-dimensional representations of Nusselt number $Nu_x = -\frac{\bar{x}}{k} \frac{(k + k_d)}{(T_f - T_{\infty,0})} \left[\frac{\partial T}{\partial y} \right]_{y=0}$

and skin friction coefficient $C_f = \frac{2}{\rho u_*^2} \left[\mu \frac{\partial u}{\partial y} \right]_{y=0}$ are

$$\frac{Nu_{\bar{x}}}{Ra^{\frac{1}{2}}} = - [Ds f'(\xi, 0) + 1] \theta'(\xi, 0), \quad \frac{1}{2} \frac{Ra^{\frac{1}{2}}}{Pr} C_f = f''(\xi, 0) \tag{9}$$

Here u_* and μ denote characteristic velocity and dynamic viscosity respectively, k_e (the effective thermal conductivity of the medium) is the sum of k_d (the dispersion thermal conductivity) and k (the molecular thermal conductivity), and Pr denotes the Prandtl number.

Numerical Solutions

The flow Eq. (6) accompanied with the energy Eq. (7) and BCs(8), constitute highly complex non-linear non-homogeneous system of PDEs and closed-form solutions for these kind of systems cannot be obtained. Therefore, the Eqs. (6)– (7) together with the BCs (8) are

solved efficiently with local non-similarity technique and spectral local linearization method (SLLM). Combination of these methods has been proved to be appropriate and assures precise outcome for complex parabolic equations. The detailed explanations of these approaches and their implementations are given below:

Local Non-Similarity Procedure

The approach given by Sparrow and Yu [31], named as local similarity and non-similarity technique, is used to obtain the system of ODEs by employing the three levels of truncation. When $\xi \ll 1$, the preliminary approximation is found from the local similarity equations and insignificant terms involving $\xi \frac{\partial}{\partial \xi}$ are removed. Consequently the local similarity equations for the first level truncation of Eqs.(6)-(8) are

$$\left[n (f')^{n-1} + 2 Gr^* f' \right] f'' - (2\alpha_1\theta + 1)\theta' = 0 \tag{10}$$

$$\theta'' + (f''\theta' + f'\theta'') Ds + \left(\frac{\xi}{\xi + 1} + 0.5 \right) f\theta' - S_T \xi f' = 0 \tag{11}$$

and the corresponding BCs are

$$\begin{aligned} f(\xi, 0) = 0, \quad \theta'(\xi, 0) + Bi \xi^{\frac{1}{2}} [1 - \theta(\xi, 0) - S_T \xi] = 0, \\ f'(\xi, \eta) \rightarrow 0, \quad \theta(\xi, \eta) \rightarrow 0 \text{ as } \eta \rightarrow \infty. \end{aligned} \tag{12}$$

The second level truncation involves the use of new variables $U = \frac{\partial f}{\partial \xi}$, $V = \frac{\partial \theta}{\partial \xi}$, by which the local non-similarity non-linear ODEs are derived to get the previously omitted terms. Hence, updated governing equations are boundary conditions are

$$\left[n (f')^{n-1} + 2 Gr^* f' \right] f'' - (2\alpha_1\theta + 1)\theta' = 0 \tag{13}$$

$$\theta'' + (f''\theta' + f'\theta'') Ds + \left(\frac{\xi}{\xi + 1} + 0.5 \right) f\theta' - S_T \xi f' - \xi V f' + \xi U \theta' = 0 \tag{14}$$

$$(3\xi + 1)f(\xi, 0) + 2(\xi + 1)\xi U(\xi, 0) = 0,$$

$$\theta'(\xi, 0) + Bi \xi^{\frac{1}{2}} [1 - S_T \xi - \theta(\xi, 0)],$$

$$f'(\xi, \eta) \rightarrow 0, \quad \theta(\xi, \eta) \rightarrow 0 \text{ as } \eta \rightarrow \infty. \tag{15}$$

Finally, in last truncation level, Eqs.(13)-(15) are differentiated in respect of ξ and all partial derivatives of U and V are removed. Therefore, the final equations are

$$\begin{aligned} n (f')^{n-1} U'' + n(n - 1) (f')^{n-2} f'' U' + 2Gr^*(U'' f' + f'' U') \\ - V' - 2\alpha_1(\theta V' + V\theta') = 0 \end{aligned} \tag{16}$$

$$\begin{aligned} V'' + Ds(f'V'' + f''V') + \left(\frac{1}{2} + \frac{\xi}{\xi + 1} \right) fV' - f'V + \xi UV' - \xi U'V \\ + Ds(U''\theta' + U'\theta'') + \left(\frac{1}{2} + \frac{\xi}{\xi + 1} \right) U\theta' - S_T f' - \xi S_T U' + \theta'U + \frac{1}{(\xi + 1)^2} f\theta' = 0 \end{aligned} \tag{17}$$

with boundary conditions

$$\begin{aligned}
 3f(\xi, 0) + (7\xi + 3)U(\xi, 0) &= 0, \\
 V'(\xi, 0) - Bi\xi^{\frac{1}{2}}V(\xi, 0) + 0.5Bi\xi^{-\frac{1}{2}}[1 - \theta(\xi, 0)] - 1.5Bi\xi^{\frac{1}{2}}S_T, & \quad (18) \\
 U'(\xi, \eta) \rightarrow 0, \quad V(\xi, \eta) \rightarrow 0 & \text{ as } \eta \rightarrow \infty.
 \end{aligned}$$

Spectral Local Linearization Method (SLLM)

SLLM is initially developed by Motsa [32] to find the solutions of non-linear coupled ODEs. The solution procedure of this problem with SLLM consists of the following three steps: (i) first, the Eqs.(13)-(14) and Eqs.(16)-(17) are decoupled using Gauss-Seidel method and then the well-known quasi-linearization technique is used to linearize the nonlinear components of the decoupled equations; (ii) next, the Chebyshev spectral collocation method is adopted to transform the set of linearized ODEs into the set of algebraic equations in the matrix form; (iii) finally, this matrix is solved iteratively using appropriate initial solutions.

$$f''_{r+1} + a_{1,r}f'_{r+1} = K_{1,r} \tag{19}$$

$$\theta''_{r+1} + b_{1,r}\theta'_{r+1} = K_{2,r} \tag{20}$$

$$U''_{r+1} + x_{1,r}U'_{r+1} = K_{3,r} \tag{21}$$

$$V''_{r+1} + y_{1,r}V'_{r+1} + y_{2,r}V_{r+1} = K_{4,r} \tag{22}$$

where

$$\begin{aligned}
 a_{1,r} &= \frac{n(n-1)f''_r(f'_r)^{n-2} + 2Gr^*f''_r}{n(f'_r)^{n-1} + 2Gr^*f'_r}, \\
 K_{1,r} &= \frac{\theta'_r + 2\alpha_1\theta_r\theta'_r + n(n-1)f''_r(f'_r)^{n-1} + 2Gr^*f''_rf'_r}{n(f'_r)^{n-1} + 2Gr^*f'_r}, \\
 b_{1,r} &= \frac{Ds f''_{r+1} + (\frac{1}{2} + R) f_{r+1} + \xi U_r}{1 + Ds f'_{r+1}}, \\
 K_{2,r} &= \frac{\xi S_T f'_{r+1} + \xi f'_{r+1} V_r}{1 + Ds f'_{r+1}}, \\
 x_{1,r} &= \frac{n(n-1)(f'_{r+1})^{n-2} f''_{r+1} + 2Gr^* f''_{r+1}}{2Gr^* f'_{r+1} + n(f'_{r+1})^{n-1}}, \\
 K_{3,r} &= \frac{V'_r + 2\alpha_1\theta'_{r+1}V_r + 2\alpha_1\theta_{r+1}V'_r}{n(f'_{r+1})^{n-1} + 2Gr^* f'_{r+1}}, \\
 y_{1,r} &= \frac{Ds f''_{r+1} + (\frac{1}{2} + R) f_{r+1} + \xi U_{r+1}}{1 + Ds f'_{r+1}}, \quad y_{2,r} = \frac{-f'_{r+1} - \xi U'_{r+1}}{1 + Ds f'_{r+1}}, \\
 K_{4,r} &= \frac{-Ds(U'_{r+1}\theta''_{r+1} + U''_{r+1}\theta'_{r+1}) - (\frac{3}{2} + R)U_{r+1}\theta'_{r+1} + \xi S_T U'_{r+1} + S_T f'_{r+1} - \frac{1}{(\xi+1)^2} f_{r+1}\theta'_{r+1}}{1 + Ds f'_{r+1}},
 \end{aligned}$$

with linearized boundary conditions

$$\begin{aligned}
 f_{r+1}(\xi, 0) &= -\frac{2\xi(\xi + 1)}{3\xi + 1}U_r(\xi, 0), \\
 \theta'_{r+1}(\xi, 0) - \xi^{\frac{1}{2}}Bi\theta_{r+1}(\xi, 0) &= -Bi\xi^{\frac{1}{2}} + Bi\xi^{\frac{3}{2}}S_T, \\
 U_{r+1}(\xi, 0) &= -\frac{3}{7\xi + 3}f_{r+1}(\xi, 0), \\
 V'_{r+1}(\xi, 0) - Bi\xi^{\frac{1}{2}}V_{r+1}(\xi, 0) &= -\frac{1}{2}Bi\xi^{-\frac{1}{2}} + \frac{1}{2}Bi\xi^{-\frac{1}{2}}\theta_{r+1}(\xi, 0) + \frac{3}{2}Bi\xi^{\frac{1}{2}}S_T, \\
 f'_{r+1}(\xi, \eta) \rightarrow 0, \theta_{r+1}(\xi, \eta) \rightarrow 0, U'_{r+1}(\xi, \eta) \rightarrow 0, V_{r+1}(\xi, \eta) \rightarrow 0, & \text{ as } \eta \rightarrow \infty.
 \end{aligned}
 \tag{23}$$

The matrix representation of Eqs.(19)-(22) can be given as

$$\begin{aligned}
 A_1 F &= B_1 \\
 A_2 \Theta &= B_2 \\
 A_3 U &= B_3 \\
 A_4 V &= B_4
 \end{aligned}$$

where

$$\begin{aligned}
 A_1 &= D^2 + \text{diag}(a_{1,r})D, & B_1 &= K_{1,r} \\
 A_2 &= D^2 + \text{diag}(b_{1,r})D, & B_2 &= K_{2,r} \\
 A_3 &= D^2 + \text{diag}(x_{1,r})D, & B_3 &= K_{3,r} \\
 A_4 &= D^2 + \text{diag}(y_{1,r})D + \text{diag}(y_{2,r})I, & B_4 &= K_{4,r}
 \end{aligned}$$

where I is $(N_x + 1)^{th}$ order identity matrix and F, Θ, U and V are the vectors containing f, θ, U and V values evaluated at the Gauss - Lobatto (collocation) points. The subsequent system of algebraic equations which are represented in the matrix form along with the BCs(23) are solved iteratively by making use of appropriate initial approximations to analyze the fluid flow behaviour.

Results and Discussion

This section includes the discussion of results attained by solving Eqs.(6)–(7) along with BCs(8) using the combined methods explained above for various physically reliable values of different parameters. All computations involved in this paper are done in MATLAB by taking 50 collocation points in η -direction (*i.e.* $N_x = 50$) and $L_x = 10$ is fixed in the η -direction to get the asymptotic nature at infinity. The convergence property is shown by using the following expressions for the error in fluid velocity and fluid temperature at $(r + 1)^{th}$ level

$$\begin{aligned}
 E_f &= \max||f_{r+1,i} - f_{r,i}||_{\infty}, & 0 \leq i \leq N_x, \\
 E_{\theta} &= \max||\theta_{r+1,i} - \theta_{r,i}||_{\infty}, & 0 \leq i \leq N_x.
 \end{aligned}$$

Figures 2a–3b display the variations in the norm of residual error with iterations for Eqs. (13) and (14) with different ξ . The residual error is decreased with increase in iterations and its very less quantity in all the cases shows the convergence and accuracy of the method. Hence, the validation of this spectral local linearisation method is concluded.

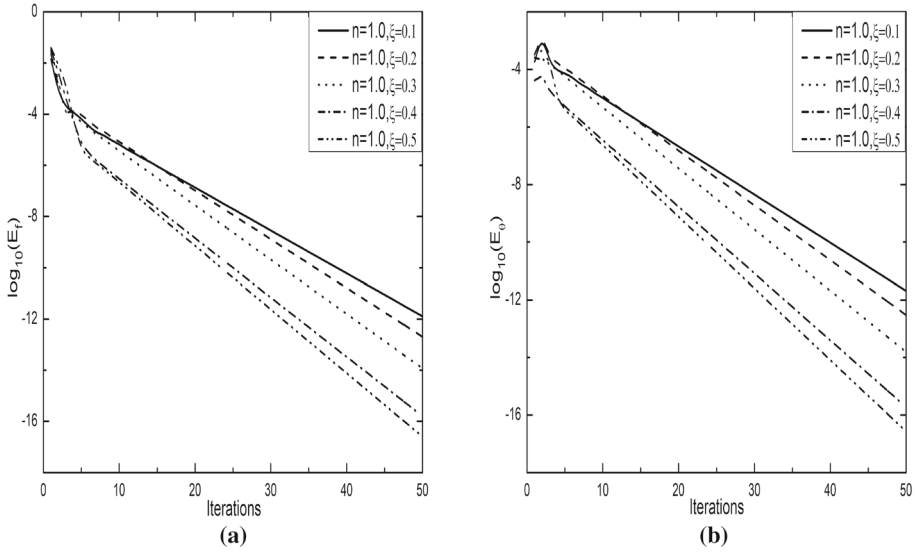


Fig. 2 Residual errors over iterations for Newtonian fluid when $Ds = 1.0$, $\alpha_1 = 0.1$, $Gr^* = 0.01$, $Bi = 1.0$, $S_T = 0.01$

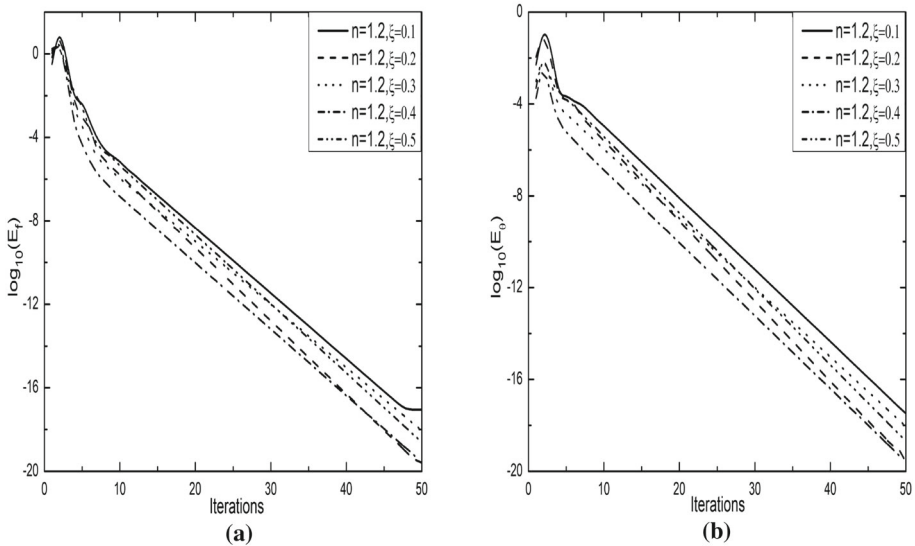


Fig. 3 Residual errors over iterations for non-Newtonian fluid when $Ds = 0.5$, $\alpha_1 = 0.1$, $Gr^* = 0.01$, $Bi = 1.0$, $S_T = 0.01$

Further, to check the accuracy of computations and the exactness of formulation, results of this problem in the case of wall temperature condition ($\theta(\xi, \eta) = 1$ as $Bi \rightarrow \infty$) for vertical plate (i.e. $\xi \rightarrow 0$) when $Ds = 0$, $\alpha_1 = 0$ and $S_T = 0$, are also compared with the results of Plumb and Huenefeld [33] and the exact results (see Nakayama *et al.* [34] and citations therein) for the Newtonian fluid case. These comparisons are coinciding at a large extent as displayed in Table 1. The results of this problem when $\xi \rightarrow 0$, $n = 1$, $\alpha_1 = 0$, $S_T = 0$ and

Table 1 Comparative analysis of $-\theta'(\xi, 0)$ for different values of Gr^* when $\xi \rightarrow 0, Ds = 0, \alpha_1 = 0, S_T = 0, Bi \rightarrow \infty$ and $n = 1$ (Newtonian fluid)

Gr^*	Present	Exact	Plumb [33]
0	0.44390437	0.4439	0.44390
0.01	0.44231590	0.4423	0.44232
0.1	0.42968906	0.4297	0.42969
1	0.36616650	0.3662	0.36617
10	0.25748252	0.2513	0.25126
100	0.16190872	0.1519	0.15186

Table 2 The non-dimensional velocities, temperatures, Nusselt number and skin friction coefficients for various values of ξ when $Gr^* = 1.0, Ds = 0.5, \alpha_1 = 1.0, Bi = 1.0, S_T = 0.01$ and $n=0.8$ (psudoplastic fluids)

ξ	$f'(\xi, 0)$	$\theta(\xi, 0)$	$\frac{Nu_{\bar{x}}}{Ra^{\frac{1}{2}}}$	$\frac{1}{2} \frac{Ra^{\frac{1}{2}}}{Pr} C_f$
0.1	0.4497	0.4778	0.2019	-0.1734
0.2	0.5169	0.5375	0.2592	-0.2155
0.3	0.5513	0.5727	0.2965	-0.2447
0.4	0.5730	0.5984	0.3235	-0.2683
0.5	0.5894	0.6185	0.3474	-0.2877
0.6	0.6033	0.6341	0.3628	-0.3035
0.7	0.6200	0.6428	0.3838	-0.3128

Table 3 The non-dimensional velocities, temperatures, Nusselt number and skin friction coefficients for various values of ξ when $Gr^* = 1.0, Ds = 0.5, \alpha_1 = 1.0, Bi = 1.0, S_T = 0.01$ and $n=1.2$ (dilatant fluids)

ξ	$f'(\xi, 0)$	$\theta(\xi, 0)$	$\frac{Nu_{\bar{x}}}{Ra^{\frac{1}{2}}}$	$\frac{1}{2} \frac{Ra^{\frac{1}{2}}}{Pr} C_f$
0.1	0.4896	0.4561	0.2137	-0.1626
0.2	0.5494	0.5194	0.2728	-0.2017
0.3	0.5830	0.5551	0.3126	-0.2277
0.4	0.6062	0.5798	0.3430	-0.2474
0.5	0.6239	0.5986	0.3677	-0.2632
0.6	0.6382	0.6138	0.3884	-0.2764
0.7	0.6501	0.6265	0.4063	-0.2877

$Bi \rightarrow \infty$, are tuned with the findings of Murthy and Singh [35], who investigated the impact of thermal dispersion parameter in natural convection. Further, the behavior of temperature and velocity profiles along with the skin friction coefficient and heat transfer rate for various values of streamwise coordinate ξ is given in tabular form for pseudoplastic fluid and dilatant fluid in Table2 and Table3 respectively. From these results, it is self evident that the solutions are not similar. This flow model reveals some interesting observations regarding heat transfer and boundary layer in the practically feasible range of important parameters and these are very useful in various emerging applications.

Impact of Biot Number (Bi)

The variations in the non-dimensional velocities, temperatures, heat transfer rates and skin friction coefficients for different Bi are portrayed graphically in Figs. 4a–4d where all other

parameters are given fixed values. Bi is defined as the proportion of internally heated resistance in the truncated cone surface to the boundary layer heated resistance. Figure 4a depicts the fluid velocity increments with higher values of Bi and dilatant fluid is more influenced in comparison of pseudoplastic fluid. In Fig. 4b, the influence of Bi on temperature profiles is displayed which shows that the higher values of temperature are obtained with the increment in Biot number. It is clear from this figure that the temperature is more for both the fluids when the surface is subjected to wall temperature condition (i.e., $\theta(\xi, 0) = 1 - \xi S_T$ which is obtained when $Bi \rightarrow \infty$) in comparison to the convectively heated surface (as shown in Boundary condition (8)). The variations in Nusselt number with non-linear convection parameter α_1 for various values of Biot number are shown in Fig. 4c. There is domination of dilatant fluid over pseudoplastic fluid and higher rate of heat transfer is noticed with increment in Bi . Similarly, in Fig. 4d, the changes in skin friction coefficient with α_1 for different values of Bi are displayed. Less negative values are obtained for dilatant fluid with an increment of Bi and this negativity increases with Biot number increment. This type of analysis where the temperature of surface is fixed in later stage, may be very useful in many applications because if the surface temperature is fixed initially, it may further result into damage of materials involved in the experiment or even in industry.

Impact of Thermal Stratification Parameter (S_T)

In the Figs. 5a–5d, the significance of S_T on non-dimensional velocities of the fluid flow, temperatures, heat transfer rates and skin friction coefficients are depicted. There are decrements in the velocity and temperature profiles in the case of increasing values of stable stratification (i.e., for $S_T > 0$) for both dilatant and pseudoplastic fluids. Due to S_T increment, density of the fluid is increased which results the decrement in the convective flow and so the velocity profiles are decreased and the effect is less for pseudoplastic fluid. Also, in the presence of S_T , the temperature variation between the surface of the truncated cone and the marginal fluid decreases, which thickens the thermal boundary layer resulting into temperature profile decrement. In Fig. 5c, the impact of stratification on Nusselt number with α_1 is shown for dilatant and pseudoplastic fluids. Increase in S_T values results into the decrement of Nusselt number for both the fluids. Nusselt number is noticed to be less in the case of pseudoplastic fluids. Fig. 5d shows the impact of stratification on the skin friction coefficient with α_1 and increment in S_T makes skin friction values less negative for dilatant and pseudoplastic fluids and there is rapid variation with α_1 values.

Impact of Thermal Dispersion Parameter (D_s)

The variations in the non-dimensional velocities, temperatures, Nusselt number and skin friction coefficients are depicted in Figs. 6a–6d. Thermal dispersion raises the potency of non-uniform pore level velocities on the temperature field in a certain porous medium. In addition, the importance of integrated variations in temperature and velocity profiles to the heat transportation can also be seen with the help of thermal dispersion. It is found from the Fig. 6a that there is increment in velocities when thermal dispersion parameter is present in the case of dilatant and pseudoplastic fluids. Likewise, Fig. 6b portrays that there is again increment in the temperature profiles for non-zero values of D_s . Due to higher flow velocities in the porous medium, thermal dispersion dominates molecular diffusion. Hence, a detailed analysis must be given about its impact on heat transfer properties in this study. In view of this, the impact of D_s with α_1 on Nusselt number is shown in Fig. 6c. With enhanced values

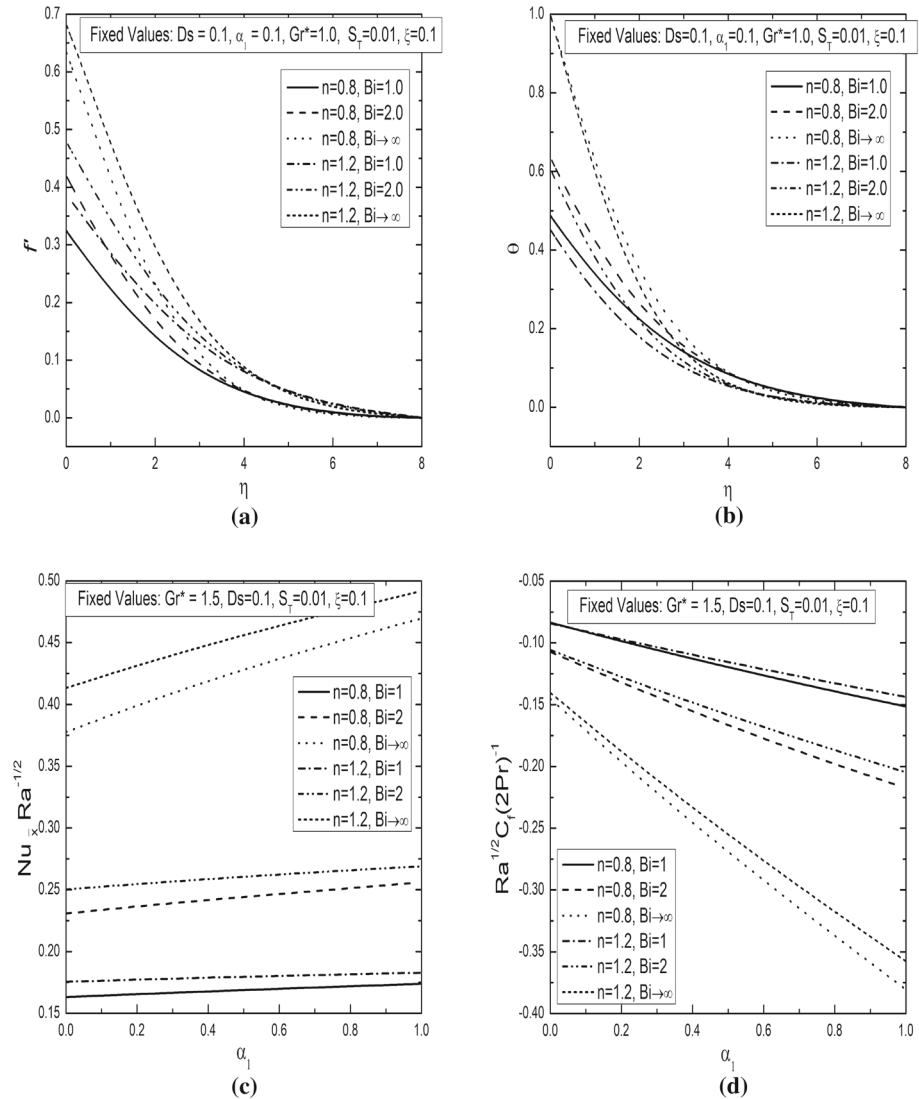


Fig. 4 The **a** non-dimensional velocity, **b** non-dimensional temperature, **c** non-dimensional Nusselt number and **d** non-dimensional skin friction coefficient profiles for different values of n and Bi

of Ds , the heat transfer is also enhanced for both dilatant and pseudoplastic fluids. The values for dilatant fluid are found to be more. The influence of Ds on the skin friction coefficient with α_1 is displayed in Fig. 6d. When Ds is increased, less negative skin friction is observed for the two fluids. The magnitude of Ds is higher for pseudoplastic fluids than dilatant fluids.

Impact of Non-Linear Convection Parameter (α_1)

The effect of α_1 on the dimensionless velocities and temperatures are displayed in Figs. 7a–7b. The non-linear convection parameter shows a non-linear relationship between temperature

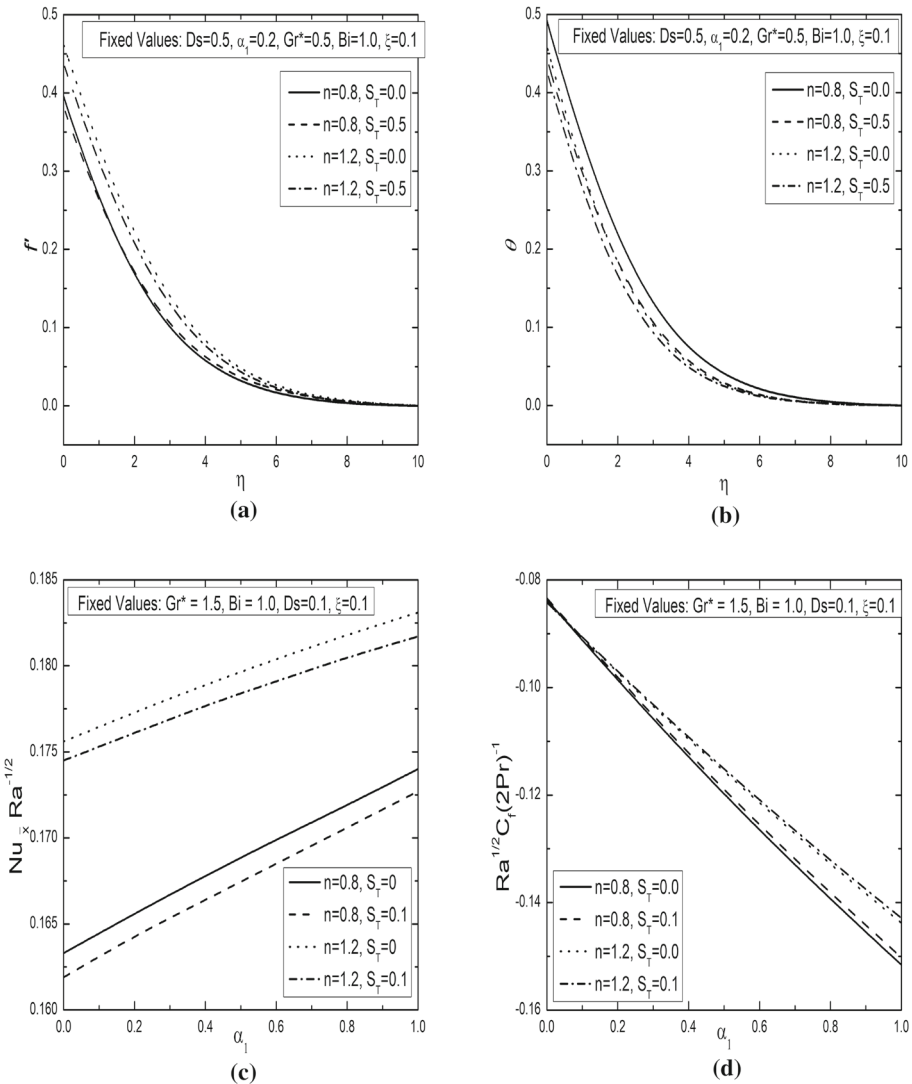


Fig. 5 The **a** non-dimensional velocity, **b** non-dimensional temperature, **c** non-dimensional Nusselt number and **d** non-dimensional skin friction coefficient profiles for different values of n and S_T

and density. Physically, $\alpha_1 > 0$ refers the expression $T_f > T_\infty$, so the truncated cone surface gives significant amount of heat to the fluid flow region. The presence and absence of α_1 is taken to analyse its influence when other parameters are assigned specific values. Fig. 7a displays that the presence of α_1 makes velocity to increase and this effect is less for pseudoplastic fluid. Fig. 7b displays the temperature decrements in the presence of α_1 for both the fluids and these decrements are found to be more in the case of pseudoplastic fluid. As α_1 increases, from Figs. 4c–4d and Figs. 6c–6d, it is evident that the Nusselt number and skin friction are less affected for pseudoplastic fluids than dilatant fluids in the presence/absence of either convective boundary condition or thermal dispersion. With the increment in α_1 , the

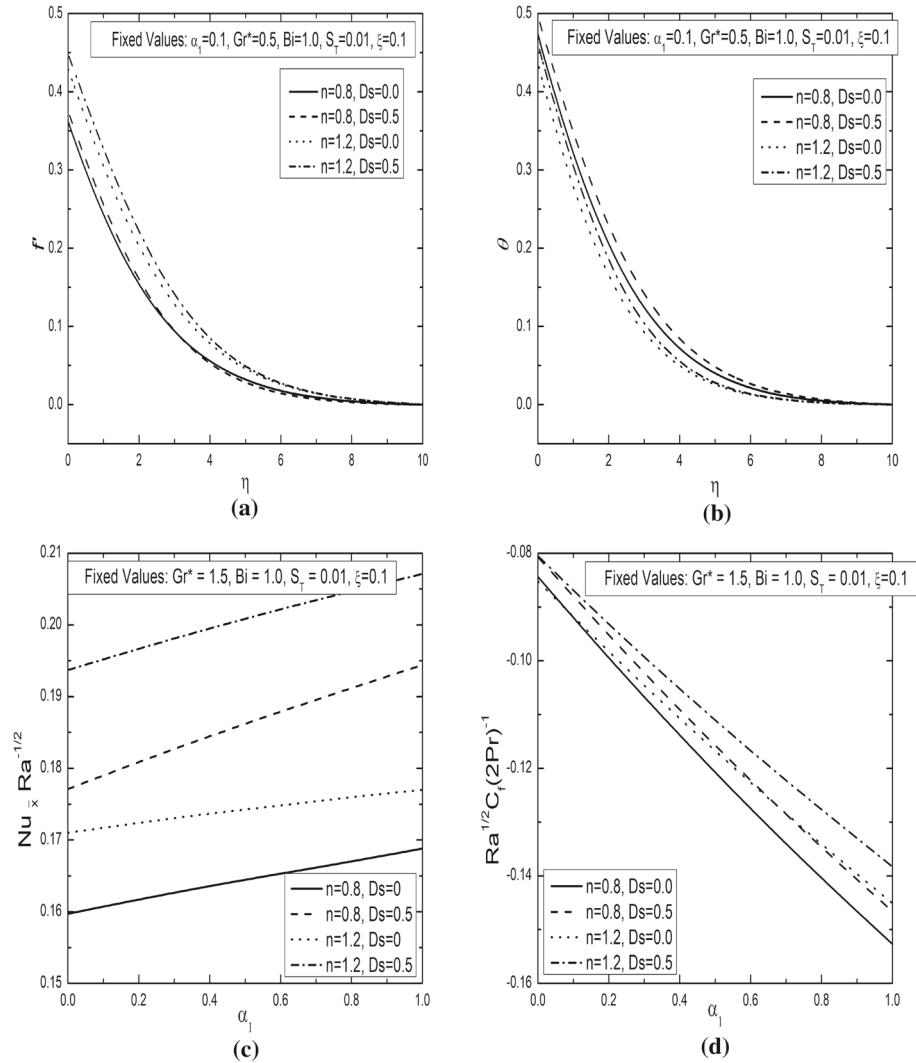


Fig. 6 The **a** non-dimensional velocity, **b** non-dimensional temperature, **c** non-dimensional Nusselt number and **d** non-dimensional skin friction coefficient profiles for different values of n and D_s

Nusselt number is identified to be more for pseudoplastic fluids when compared to dilatant fluids with/without S_T as displayed in Fig. 5c. The behaviour of skin friction coefficient is noticed to be opposite to that of the Nusselt number as shown in Fig. 5d with the enhancement in the parameter α_1 .

Conclusion

The impacts of Biot number, thermal dispersion and non-linear convection on the thermally stratified power-law fluid over the truncated cone situated in a non-Darcy porous medium,

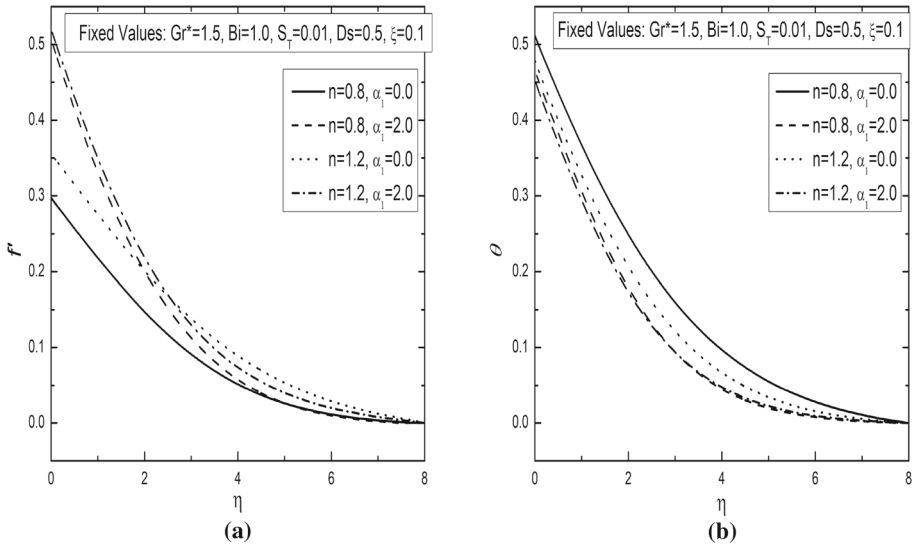


Fig. 7 The **a** non-dimensional velocity and **b** non-dimensional temperature distributions for different values of n and α_1

are discussed in this work. The consideration of these effects increased the number of non-dimensional parameters and hence increased the non-linear complexity of this problem. So, the governing equations are handled by local non-similarity and spectral local linearization approaches. These kinds of analyses play very important part in the area of polymeric mixtures maintained at very high temperatures, aerosol technology etc., and these all are related to temperature-dependent density. In future work, one can try to solve boundary layer equations related to this model for fractional order cases by following the papers [36,37] which involve a method free from restrictive cases or linearization and it may provide the exact solution in terms of a uniformly convergent series. The decisive observations for this work can be itemized as:

- The velocities, temperatures and Nusselt number are increased for larger Bi but the skin friction coefficient is reduced for pseudoplastic and dilatant fluids.
- Thermal stratification parameter influences temperature, velocity and rate of heat transfer in a similar way and all these face decrement with higher values of S_T . But, the different trend is seen in the skin friction coefficient case.
- The effect of Ds on the temperature, velocity, heat transfer rate and skin friction coefficient is all positive as all these profiles are increased with its presence.
- The impact of non-linear convection parameter α_1 on velocity and temperature profiles is opposite in nature as its presence gives increment in the velocity profiles, and decrement in the temperature profiles.

References

1. Liu, W., Li, X., Zhao, Q.: A two-grid expanded mixed element method for nonlinear non-Fickian flow model in porous media. *Int. J. Comput. Math.* **91**, 1299–1314 (2014)
2. Vafai, K.: *Hand Book of Porous Media*. Basel, Marcel Dekker Inc, New York (2000)

3. Pop, I., Ingham, D.B.: *Convective Heat Transfer: Mathematical and Computational Modeling of Viscous Fluids and Porous Media*. Pergamon, Oxford (2001)
4. Nield, D.A., Bejan, A.: *Convection in Porous Media*. Springer, New-York (2017)
5. Shenoy, A.V.: Darcy-Forchheimer natural, forced and mixed convection heat transfer in non-Newtonian power-law fluid-saturated porous media. *Transp. Porous Media* **11**, 219–241 (1993)
6. Cheng, C.Y.: Double-diffusive natural convection along a vertical wavy truncated cone in non-Newtonian fluid saturated porous media with thermal and mass stratification. *Int. Commun. Heat Mass Transf.* **35**, 985–990 (2008)
7. Mandal, P.K., Chakravarty, S., Mandal, A.: Numerical study of the unsteady flow of non-Newtonian fluid through differently shaped arterial stenoses. *Int. J. Comput. Math.* **84**, 1059–1077 (2007)
8. Khidir, A.A., Narayana, M., Sibanda, P., Murthy, P.V.S.N.: Natural convection from a vertical plate immersed in a power-law fluid saturated non-Darcy porous medium with viscous dissipation and Soret effects. *Afrika Matematika* **26**, 1495–1518 (2015)
9. Kairi, R.R.: Free convection around a slender paraboloid of non-Newtonian fluid in a porous medium. *Thermal Sci.* **23**, 3067–3074 (2019)
10. Dake, J.M.K., Harleman, D.R.F.: Thermal stratification in lakes: analytical and laboratory studies. *Water Resour. Res.* **5**, 484–495 (1969)
11. Knudsen, S., Furbo, S.: Thermal stratification in vertical mantle heat-exchangers with application to solar domestic hot-water systems. *Appl. Energy* **78**, 257–272 (2004)
12. Narayana, P.A.L., Murthy, P.V.S.N., Krishna, P.V.S.S.R., Postelnicu, A.: Free convective heat and mass transfer in a doubly stratified porous medium saturated with a power-law fluid. *Int. J. Fluid Mech. Res.* **36**, 524–537 (2009)
13. Cheng, C.Y.: Combined heat and mass transfer in natural convection flow from a vertical wavy surface in a power-law fluid saturated porous medium with thermal and mass stratification. *Int. Commun. Heat Mass Transf.* **36**, 351–356 (2009)
14. Cheng, P.: Thermal dispersion effects in non-Darcian convective flows in a saturated porous medium. *Lett. Heat Mass Transf.* **8**, 267–270 (1981)
15. Plumb, O. A.: The effect of thermal dispersion on heat transfer in packed bed boundary layers in: *Proceedings of the ASME JSME Thermal Engineering Joint Conference* **2**, (1983)
16. Hong, J.T., Yamada, Y., Tien, C.L.: Effects of non-Darcian and nonuniform porosity on vertical-plate natural convection in porous media. *Trans. ASME* **109**, 356–362 (1987)
17. Kairi, R.R., Murthy, P.V.S.N.: Free convection in a thermally stratified non-Darcy porous medium saturated with a non-Newtonian fluid. *Int. J. Fluid Mech. Res.* **36**, 414–423 (2009)
18. Srinivasacharya, D., Pranitha, J., RamReddy, Ch.: Magnetic and double dispersion effects on free convection in a non-Darcy porous medium saturated with power-law fluid. *Int. J. Comput. Methods Eng. Sci. Mech.* **13**, 210–218 (2012)
19. Vasu, B., RamReddy, Ch., Murthy, P.V.S.N., Gorla, R.S.R.: Entropy generation analysis in nonlinear convection flow of thermally stratified fluid in saturated porous medium with convective boundary condition. *J. Heat Transf.* **139**, 1–21 (2017)
20. Ece, M.C., Buyuk, E.: Similarity solutions for free convection to power-law fluids from a heated vertical plate. *Appl. Math. Lett.* **15**, 1–5 (2002)
21. Yao, S., Fang, T., Zhong, Y.: Heat transfer of a generalized stretching/shrinking wall problem with convective boundary conditions. *Commun. Nonlinear Sci. Numer. Simulat.* **16**, 752–760 (2011)
22. Partha, M.K.: Nonlinear convection in a non-Darcy porous medium. *Appl. Math. Mech.* **31**, 565–574 (2010)
23. RamReddy, Ch., Naveen, P., Srinivasacharya, D.: Effects of nonlinear Boussinesq approximation and double dispersion on free convective flow of an Ostwald-de Waele power-law fluid along an inclined plate. *J. Nanofluids* **7**, 1247–1257 (2018)
24. Na, T.Y., Chiou, J.P.: Laminar natural convection over a frustum of a cone. *Appl. Sci. Res.* **35**, 409–421 (1979)
25. Gorla, R.S.R., Krishnan, V., Pop, I.: Free convection of a power-law fluid over the vertical frustum of a cone. *Int. J. Eng. Sci.* **32**, 1791–1800 (1994)
26. Cheng, C.Y.: Natural convection heat and mass transfer from a vertical truncated cone in a porous medium saturated with a non-Newtonian fluid with variable wall temperature and concentration. *Int. Commun. Heat Mass Transf.* **36**, 585–589 (2009)
27. Cheng, C.Y.: Double diffusion from a vertical truncated cone in a non-Newtonian fluid saturated porous medium with variable heat and mass fluxes. *Int. Commun. Heat Mass Transf.* **37**, 261–265 (2010)
28. Singh, P., Radhakrishnan, V., Narayan, K.A.: Non-similar solutions of free convection flow over a vertical frustum of a cone for constant wall temperature. *Ingenieur-Archiv* **59**, 382–389 (1989)

29. Christopher, R.H., Middleman, S.: Power-law flow through a packed tube. *Indust. Eng. Chem. Fundamentals* **4**, 422–426 (1965)
30. Dharmadhikari, R.V., Kale, D.D.: Flow of non-Newtonian fluids through porous media. *Chem. Eng. Sci.* **40**, 527–529 (1985)
31. Sparrow, E.M., Yu, H.S.: Local non-similarity thermal boundary-layer solutions. *Trans. ASME J. Heat Transf.* 328–334 (1971)
32. Motsa, S.S.: A new spectral local linearization method for nonlinear boundary layer flow problems. *J. Appl. Math.* **2013**, 1–15 (2013)
33. Plumb, O.A., Huenefeld, J.C.: Non-Darcy natural convection from heated surfaces in saturated porous media. *Int. J. Heat Mass Transf.* **24**, 765–768 (1981)
34. Nakayama, A., Kokudai, T., Koyama, H.: An integral treatment for non-Darcy free convection over a vertical flat plate and cone embedded in a fluid-saturated porous medium. *Warme-und Stoffubertragung* **23**, 337–341 (1988)
35. Murthy, P.V.S.N., Singh, P.: Thermal dispersion effects on non-Darcy natural convection with lateral mass flux. *Heat Mass Transf.* **33**, 1–5 (1997)
36. Jajarmi, A., Baleanu, D.: A new iterative method for the numerical solution of high-order non-linear fractional boundary value problems. *Front. Phys.* **8**, 220 (2020)
37. Jajarmi, A., Baleanu, D.: On the fractional optimal control problems with a general derivative operator. *Asian J. Control* 1–10 (2019)

Publisher's Note Springer Nature remains neutral with regard to jurisdictional claims in published maps and institutional affiliations.